Materials Chemistry and Physics 124 (2010) 861–864

Contents lists available at ScienceDirect

Materials Chemistry and Physics

journal homepage: www.elsevier.com/locate/matchemphys

# Synthesis of carbon-encapsulated iron carbide/iron nanoparticles from phenolic-formaldehyde resin and ferric nitrate

Mu Zhao [a,b], Huaihe Song [a,*]

[a] State Key Laboratory of Chemical Resource Engineering, Beijing University of Chemical Technology, Beijing 100029, PR China
[b] Chinergy CO. Ltd., Beijing 100084, PR China

ARTICLE INFO

*Article history:*
Received 21 October 2009
Received in revised form 23 June 2010
Accepted 3 August 2010

*Keywords:*
Nanostructures
Oxides
Polymers

ABSTRACT

Carbon-encapsulated iron carbide/iron nanoparticles have been synthesized on a large scale by the heat treatment of thermal plastic phenolic-formaldehyde resin with the aid of ferric nitrate. The effects of heating temperature on the morphologies and structures of carbonized products were investigated using transmission electron microscope, high-resolution transmission electron microscope and X-ray diffraction measurements. The products with diameter distribution of 20–100 nm consisted mainly of spheroidal nanoparticles separated by hollow onion-like carbon nanoparticles.



## 1. Introduction

Since Iijima's landmark paper on carbon nanotubes [1], extensive experimental research has been performed to produce new carbon nanostructures, such as carbon nanohorns [2,3] and nanoparticles [4,5]. Recently, the synthesis of carbon-encapsulated metal nanoparticles has been deeply attracted by researchers due to their unique optical [6], magnetic [7], electronic [8] and catalytic [9,10] properties which are undoubtedly important for the evolution and revolution of the nanotechnologies.

As well known, nanometric metal particles can suffer from a rapid environmental degradation (such as oxidation and hydrolysis), because of a high chemical reactivity originated from the high surface area to volume ratio of the particle, which will severely impose limitations to their industrial applications. The carbon encapsulation, as an air-stable material, is one of the best solutions, because it is chemically stable, cheap and light. Carbon shells of Fe/C core–shell objects can effectively isolate the particles from each other [11] and protect the core against environmental degradation, although they show relatively defective structures. Carbon shells can be thinned/removed by hydrogen or oxygen gas when it is desired [12]. The core structures of carbon-encapsulated metal nanoparticles are classed into a metallic phase and a carbide phase.

Various techniques have been developed for synthesizing carbon-encapsulated metal nanoparticles, such as arc discharge [13,14], high-temperature treatment [15] and plasma-enhanced chemical vapor deposition [16]. These approaches are generally difficult to obtain carbon-encapsulated metal nanoparticles in a large quantity, and most significantly, they need large energy input to facilitate a gradual reorganization of the raw carbon materials which is the limitation for large-scale preparation and applications.

In the previous experiment, carbon-encapsulated nanoparticles were prepared in our laboratory with a pressurized method, using durene, petroleum residue and aromatic heavy oil as carbon raw materials [17–19]. In this manuscript, we report a new, simple and effective technique to synthesize carbon-encapsulated iron carbide/iron nanoparticles in large quantities, because thermosetting phenolic-formaldehyde (PF) resin has high carbonization yield through eliminating small molecules at high temperature and atmospheric pressure.

## 2. Experimental

A phenolic resin (purchased from Tianjin Resin Company), condensed by phenol and formaldehyde with the aid of hydrochloric acid, was chosen as the starting carbon precursor. Apparently, it is a yellow solid possessing 300–500 polymeric units and melting point >75 °C. Ferric nitrate ($Fe(NO_3)_3{\cdot}9H_2O$, FN, analytical pure grade) was chosen as the catalyst precursor.

Defined amounts of FN and PF resin, as molar ratio 1:16, were dissolved and mixed homogeneously in ethanol, which was then evaporated to get the solid mixture. The mixture of solid powder containing FN, hexamethylenetetramine (14 wt%) and acetone was vibrated at an ultrasonic bath for 20 min. After eliminating acetone at 60 °C, the PF resin was cured at 150 °C for 4 h. Then the mixture containing cured PF resin and FN was carbonized from 500 to 900 °C in a nitrogen gas atmosphere. Samples for X-ray diffraction (XRD) analysis were mounted on a glass holder with 0.2 mm depth and patterns were recorded on a Rigaku D/max-2500B2+/PCX system using Cu Kα radiation (λ = 1.5406 Å) over the range of 5–90° (2θ) at room temperature. Transmission electron microscope (TEM) and high-resolution transmission electron microscope (HRTEM) typed Hitachi H-800 and JEM2010 were used to examine the carbonized materials. The samples for TEM and HRTEM observations

* Corresponding author. Tel.: +86 10 64434916; fax: +86 10 64434916.
*E-mail address:* songhh@mail.buct.edu.cn (H. Song).

0254-0584/$ – see front matter © 2010 Elsevier B.V. All rights reserved.
doi:10.1016/j.matchemphys.2010.08.011

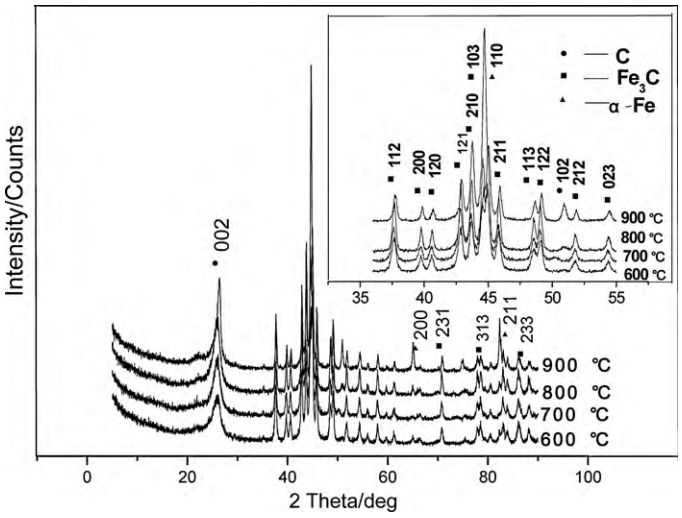


**Fig. 1.** XRD patterns of carbon-encapsulated iron carbide/iron nanoparticles.

were prepared by dispersing the products in ethanol for 15 min with an ultrasonic bath and then a few drops of the resulting suspension were placed on a copper grid.

## 3. Results and discussion

XRD characterization was performed to validate the corresponding core-shell nanostructure. Fig. 1 presents the patterns of the products carbonized at 600, 700, 800 and 900 °C. The peaks at 37.6°, 39.7°, 40.9°, 43.02°, 43.52°, 44.96°, 46.03°, 48.63°, 49.26°, 51.87°, 54.58°, 70.98°, 78.71° and 83.30° can be identified as the (1 1 2), (2 0 0), (1 2 0), (1 2 1), (2 1 0), (1 0 3), (2 1 1), (1 1 3), (1 2 2), (2 1 2), (0 2 3), (2 0 0), (2 3 1), (3 1 3) and (2 3 3) planes of $Fe_3C$; those at 44.96°, 65.02° and 82.13° can be ascribed to the (1 1 0), (2 0 0) and (2 1 1) reflections of α-Fe. It is evident that $Fe_3C$ and α-Fe coexist with well-crystallized structure [19]. The peaks around 26.38° assigned to the diffraction of (0 0 2) plane of encapsulating carbon sheets turn gradually sharper, and the corresponding interlayer spacing values (0.3483, 0.3412, 0.3381 and 0.3365 nm) become smaller with the temperature increasing from 600, 700 and 800 to 900 °C, suggesting the higher graphitization degree. The peaks of product carbonized at 600 °C are broader and lower indicating a relatively small crystalline dimension, so there are more amorphous carbon and other elements such as H, O presenting.

TEM images of carbon-encapsulated iron carbide/iron nanoparticles are shown in Fig. 2. The iron carbide/iron nanoparticles show a darker contrast than graphitic sheets because of the higher atomic number of iron than carbon. TEM image show that the products carbonized at 600–900 °C contain spheroidal nanoparticles, which have diameter distributions between 20 and 100 nm and were separated by hollow onion-like carbon nanoparticles. Seen from Fig. 2(A–D), the higher temperature is, the iron carbide/iron nanoparticles with larger volume and fewer numbers appear gradually. The image in Fig. 2(B) clearly shows the main carbon-encapsulated iron carbide/iron nanoparticles with diameters around 30 nm. Fig. 3 presents the size distribution histogram, which corresponds to TEM images shown in Fig. 2(B). It has been found that mean particle size is 42.5 nm in good agreement with the values shown in TEM.

The products heat-treated at 500 °C are oxidized immediately when they contact air, and those treated at 600 °C are not carbonized adequately and have other elements, more 'island' structures [16] and amorphous carbon, so the carbon shells can not effectively protect the iron carbide/iron core. When the temperature is up to 800 or 900 °C, majority of products are

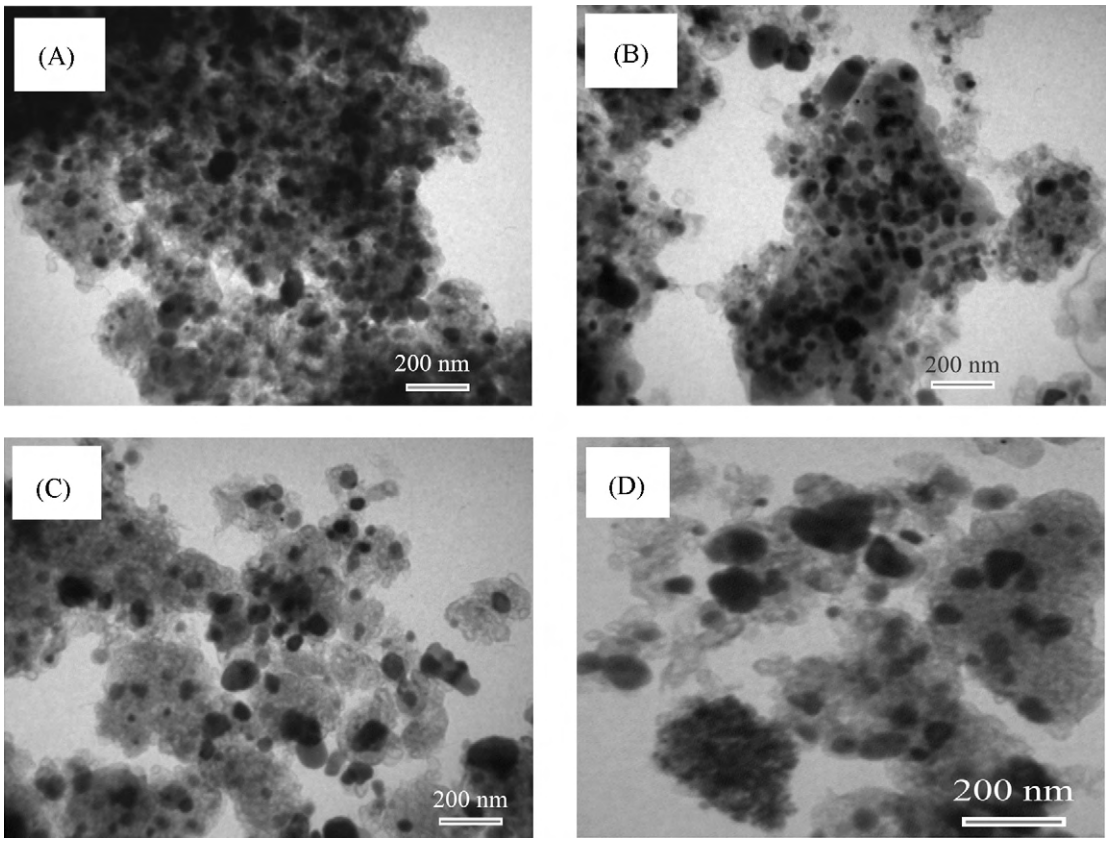


**Fig. 2.** TEM images of carbon-encapsulated iron carbide/iron nanoparticles prepared at (A) 600 °C, (B) 700 °C, (C) 800 °C and (D) 900 °C.

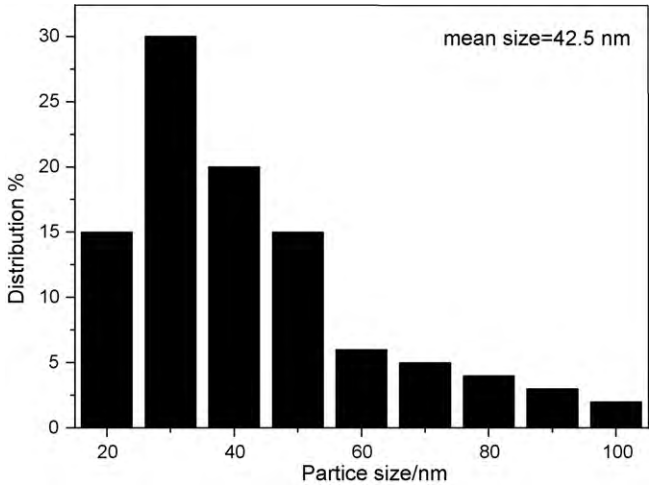


**Fig. 3.** Size distribution of carbon-encapsulated iron carbide/iron nanoparticles prepared at 700 °C.

hollow onion-like carbon nanoparticles and a small quantity of carbon-encapsulated iron carbide/iron nanoparticles with diameters around 100 nm were formed.

HRTEM (Fig. 4) analysis reveals that all of the spheroidal nanoparticles have a core–shell nanostructure with an iron carbide/iron core and carbon shells. The carbon-encapsulated iron carbide/iron nanoparticles are isolated from each other by onion-like carbon nanoparticles, seen in Fig. 4(A). The carbon shells tightly surround the core nanoparticles, few voids can be observed between the core and the shell (Fig. 4B). The shells are uniform in thickness and usually consist of 10–20 layers. The spacing of the lattice fringes is close to that of the graphite (0.3351 nm) planes. The iron carbide/iron cores are crystal related to (1 0 3) plane of $Fe_3C$ and (1 1 0) plane of α-Fe.

To validate the protection of carbon shells on the encapsulated iron carbide/iron nanoparticles, 0.1 g as-prepared products were ultrasonicated in 30 ml concentrated $HNO_3$ for 30 min, followed by filtrating, washing with distilled water, and drying at 110 °C overnight. Figs. 5 and 6 display typical TEM images and XRD patterns of carbon-encapsulated iron carbide/iron nanoparticles synthesized at 700 °C before and after oxidation, respectively. As shown in Fig. 5, the core–shell nanostructures both exist before and after $HNO_3$ treatment. As exhibited in Fig. 6, $Fe_3C$ and α-Fe are still presented with well-crystallized particles before and after oxidation. The values of $d_{002}$ are also similar with each other before (0.33412 nm) and after (0.33410 nm) oxidation. It is obvious that, although the carbon shells of the Fe–C core–shell objects showed relatively defective structure, they can still effectively protect the core against environmental degradation.

As we know, no matter how high the heat-treatment temperature is, PF as a thermosetting polymer never be converted into graphitic structure [20–23]. Through catalytic graphitization, a new formation approach was made. In the experiment, FN-doped PF resin can be readily prepared, and FN salt was accreted with PF molecules to form a molecular-scale continuous phase. Then the decomposition of FN to iron oxide occurred at 125 °C to form small

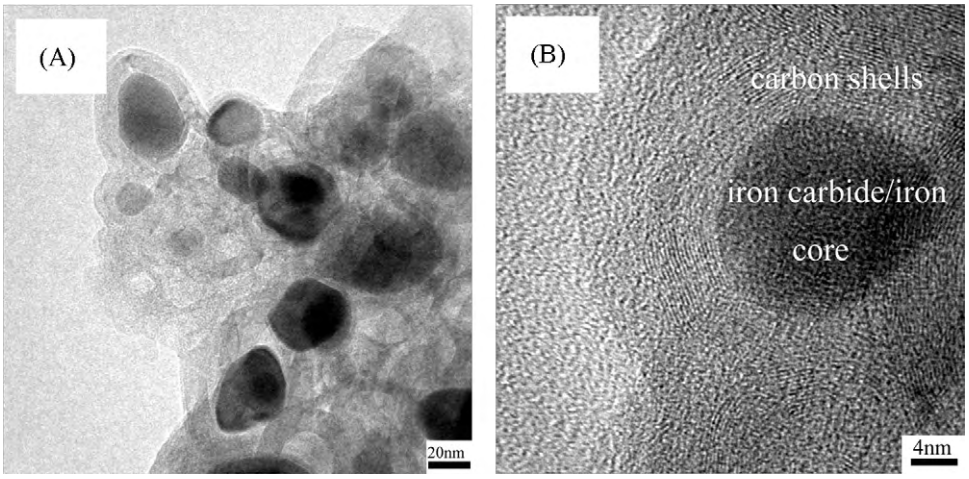


**Fig. 4.** HRTEM images of carbon-encapsulated iron carbide/iron nanoparticles synthesized at 700 °C.

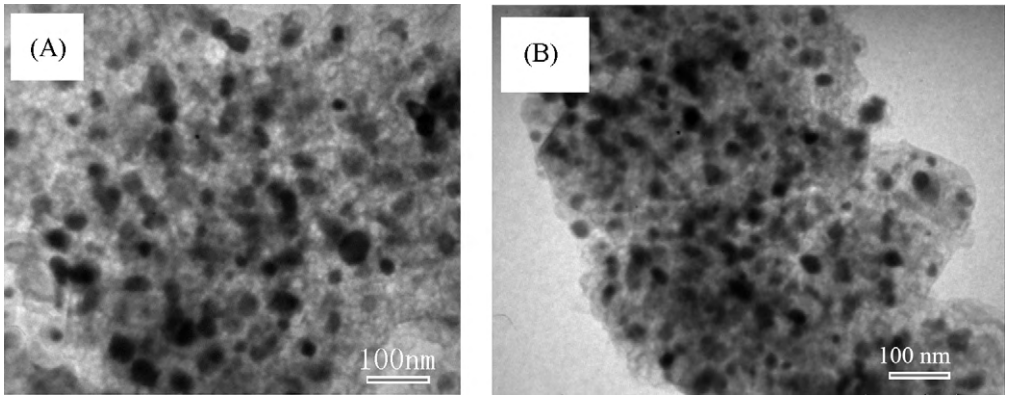


**Fig. 5.** TEM images of carbon-encapsulated iron carbide/iron nanoparticles synthesized at 700 °C before (A) and after (B) oxidation.

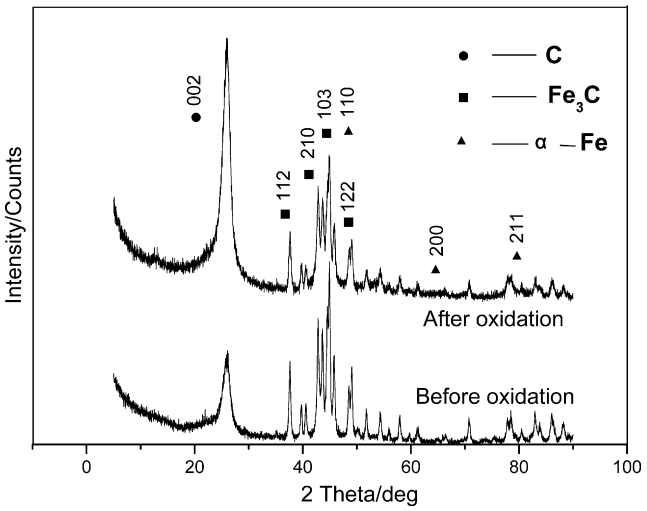


**Fig. 6.** XRD patterns of carbon-encapsulated iron carbide/iron nanoparticles synthesized at 700 °C before and after oxidation.

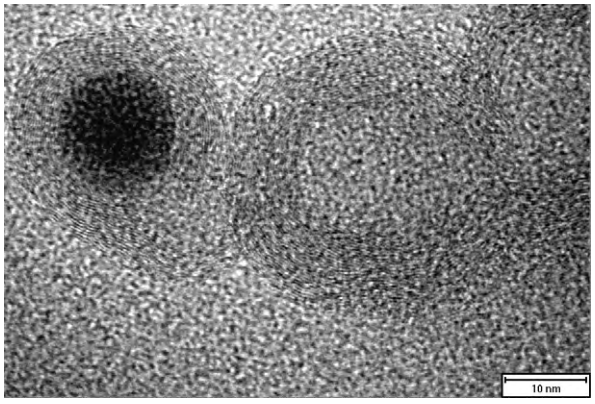


**Fig. 7.** HRTEM image of the formation stage of carbon-encapsulated iron carbide/iron nanoparticles synthesized at 900 °C.

$Fe_2O_3$ nanoparticles, which were segregated by PF molecules. After curing at 150 °C for 4 h, the linear PF molecules were cross-linked into a three-dimensional network. The carbonization resulted in higher carbon content and a closely enlaced structure. At the same time, the iron nanoparticles were gradually generated and embedded by carbon chains. With the increase of heat-treatment temperature and the elongation of maintaining time, more carbon species were dissolved into iron nanoparticles and separated out as curved graphite layers to form onion-like carbon nanoparticles when it reached a supersaturation [24]. When onion-like carbon nanoparticles were catalytically formed, temperature drops to room temperature. The iron nanoparticles have not enough time and space to agglomerate and then are encapsulated by the separated carbon species to form carbon-encapsulated iron carbide/iron nanoparticles, as shown in Fig. 7. The thickness of carbon shells is related with carbon species dissolved in iron nanoparticles. So the higher temperature is, more onion-like carbon nanoparticles and bigger and fewer carbon-encapsulated iron carbide/iron nanoparticles exist. The suitable temperature is 700 °C to synthesis carbon-encapsulated iron carbide/iron nanoparticles with diameters around 42.5 nm.

## 4. Conclusions

Large amounts of carbon-encapsulated iron carbide/iron nanoparticles with diameters of 20–100 nm were synthesized by a new method, in which PF resin was carbonized from 500 to 900 °C by the aid of iron-based catalysis. The spheroidal nanoparticles were isolated by hollow onion-like carbon nanoparticles. With the increase of temperature, the mean diameters gradually turned large. The carbon shells can effectively isolate the particles from each other and protect the core against environmental degradation. Simplicity, low cost, controllability were the key features of this approach. It will promote the practical applications of carbon-encapsulated iron carbide/iron nanoparticles in various fields.

## Acknowledgements

This work was supported by the National Natural Science Foundation of China (50572003 and 50972004) and State Key Basic Research Program of China (2006CB9326022006).

## References

[1] S. Iijima, Nature 354 (1991) 56.
[2] S. Iijima, M. Yudasaka, R. Yamada, S. Bandow, K. Suenaga, F. Kokai, K. Takahashi, Chem. Phys. Lett. 309 (1999) 165.
[3] H. Takikawa, M. Ikeda, K. Hirahara, Y. Hibi, Y. Tao, P.A. Ruiz, Physica B 323 (2002) 277.
[4] K.H. Ang, I. Alexandrou, N.D. Mathur, G.A.J. Amaratunga, S. Haq, Nanotechnology 15 (2004) 520.
[5] P.J. Si, Z.D. Zhang, D.Y. Geng, C.Y. You, X.G. Zhao, Carbon 41 (2003) 247.
[6] K. Bubke, H. Gnewuch, M. Hempstead, J. Hammer, M.L.H. Green, Appl. Phys. Lett. 71 (1997) 1906.
[7] X.L. Dong, Z.D. Zhang, S.R. Jin, W.M. Sun, X.G. Zhao, Z.J. Li, Y.C. Chuang, J. Mater. Res. 14 (1999) 1782.
[8] P.G. Collins, A. Zettl, H. Bando, A. Thess, R.E. Smalley, Science 278 (1997) 100.
[9] R. Narayanan, M.A. El-Sayed, J. Catal. 234 (2005) 348.
[10] N. Lingaiah, M.A. Uddin, A. Muto, Y. Sakata, Chem. Commun. 17 (1999) 1657.
[11] Z.F. Wang, P.E. Xiao, N.Y. He, Carbon 44 (2006) 3277.
[12] J. Nishijo, C. Okabe, O. Oishi, N. Nishi, Carbon 44 (2006) 2943.
[13] V.P. Dravid, J.J. Host, M.H. Teng, B. Eillott, J. Hwang, D.L. Johnson, T.O. Mason, J.R. Weertman, Nature 374 (1995) 602.
[14] M.H. Teng, J.J. Host, J.H. Wang, B.R. Elliott, J.R. Weertman, T.O. Mason, V.P. Dravid, D.L. Johnson, J. Mater. Res. 10 (1995) 233.
[15] P.J.F. Harris, S.C. Tsang, Carbon 36 (1998) 1859.
[16] S.H. Tsai, C.L. Lee, C.W. Chao, H.C. Shih, Carbon 38 (2000) 781.
[17] H.H. Song, X.H. Chen, Chem. Phys. Lett. 374 (2003) 400.
[18] H.H. Song, X.H. Chen, X.G. Chen, S.Y. Zhang, H.Q. Li, Carbon 41 (2003) 3037.
[19] J.P. Huo, H.H. Song, X.H. Chen, Carbon 42 (2004) 3177.
[20] P.J.F. Harris, S.C. Tsang, Philos. Mag. A 76 (1997) 667.
[21] P.J.F. Harris, Chem. Phys. Carbon 28 (2003) 9.
[22] L.L. Ban, D. Crawford, H. Marsh, J. Appl. Cryst. 8 (1975) 415.
[23] K. Kawamura, G.M. Jenkins, Nature 231 (1971) 175.
[24] M. Zhao, H.H. Song, X.H. Chen, W.T. Lian, Acta. Mater. 55 (2007) 6144.